ARTICLE NO. 79-0014R

20005
20017
60001

J80-014

Supersonic, Inviscid, Conical Corner Flowfields

Frank Marconi*
Grumman Aerospace Corporation, Bethpage, N.Y.

A computational procedure has been developed to predict the inviscid supersonic/hypersonic flowfield of conical internal corners. The prediction of internal corner flowfields can be important in the design of supersonic "box"-type inlets. The computational procedure utilizes a second-order finite-difference marching technique to approach the conical corner flow solution of Euler's equations asymptotically. These flowfields are dominated by complex shock interactions. All discontinuities, shocks, and slip surfaces are fitted with the appropriate jump conditions. The "triple" points (the interaction of three shocks and a slip surface) are also computed exactly. Computed results are compared with experimental data and the computational results of other investigators. In addition, the sensitivity of these flowfields to a number of geometric parameters is studied, and the impact of these flows on inlet performance is assessed.

I. Introduction

IN the development of supersonic and hypersonic engine inlets, a detailed prediction of the internal flowfield is critical. Inlet designers are concerned mainly with total pressure losses, flowfield nonuniformities, and flow angularities at the compressor face or flame holders (in the case of ram/scramjets). These conditions require a detailed description of the shock wave structure in three-dimensional internal flows.

This paper deals with the prediction of the inviscid, supersonic flow in two-dimensional or "box"-type inlets, as shown in Fig. 1. In particular, this paper discusses the flowfields which are generated at the four corners of this inlet (Fig. 1, station 2). The corner flowfields generate large variations in all flowfield parameters (particularly in total pressure). In the case of ram/scramjets, these corner flows are carried to the combustion chamber where they can cause nonuniform combustion, while in the case of external compression inlets (typical of Mach 2 vehicles), a normal shock will be located before the inlet lower lip so that the corner flows will interact with this shock. Here, again, the nonuniformities in total pressure generated at the inlet corners will be preserved and eventually affect the combustion.

The corner flowfields are conical if the two intersecting walls remain planar. In this situation, all flowfield variables (pressure, velocities, and entropy) are independent of the spherical radial coordinate centered at the origin of the corner flow (Fig. 1) rendering these flowfields dependent only on two space dimensions. Any fully three-dimensional computation will require conical corner flow solutions as initial conditions. In addition, the knowledge gained in a study of the conical flow problem is essential to the success of three-dimensional computations. This paper deals with conical corner flowfields of the type generated by two compressing wedges, since this configuration is typical of supersonic inlet flows.

Two possible shock configurations could be generated by the intersection of two compressive wedges. One is called a regular reflection configuration, the other a Mach disk configuration. These terms refer to the shock conditions at the intersection of the purely two-dimensional shocks from each wedge. These possibilities were investigated for a symmetrical geometry (i.e., two wedges of equal deflections); results are shown in Fig. 2. The regular reflection wave configuration has been predicted using linearized theory.[1] The Mach disk shock configuration has been shown experimentally,[2,3] and in the numerical solutions of Euler's equations using a shock capturing approach.[4-6] Figure 2 shows that for deflections above 5 deg, the only possible solution is the Mach disk shock configuration, so that linearized prediction techniques of Ref. 1 break down quite rapidly with increasing deflection angles. The conditions at both points A (triple points) and B of Fig. 2 are similar in that pressure and conical flow deflection (the flow deflection on a sphere centered at the origin) match on the high-pressure side of both these points. In addition, contact surfaces are generated at these points because of the different entropies produced by the wave systems on either side of the contact. The contact surface in the regular reflection case is due to asymmetries which do not exist in the case shown in Fig. 2. The conditions at the triple point—matching of pressure and flow deflection—are called the von Neumann conditions.[7] When the Mach number relative to the triple point is decreased below a value dependent on the

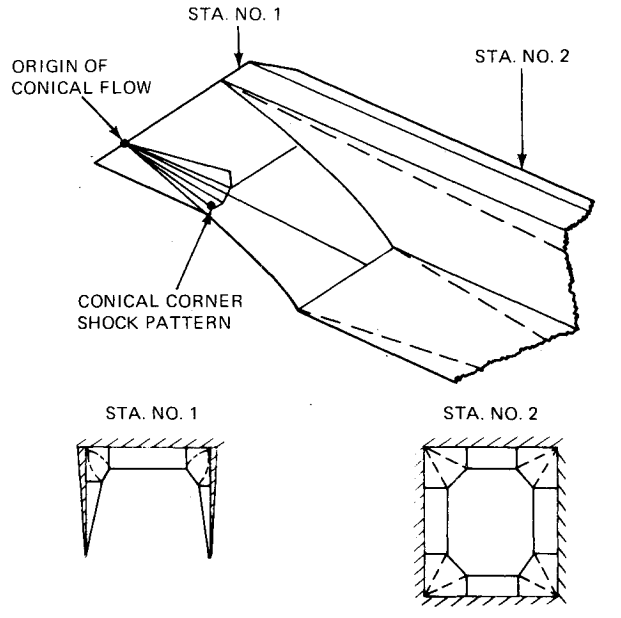

Fig. 1 "Two-dimensional" or "box"-type inlet, corner flow shock pattern.

Presented as Paper 79-0014 at the AIAA 17th Aerospace Sciences Meeting, New Orleans, La., Jan. 15-17, 1979; submitted Feb. 28, 1979; revision received June 21, 1979.

Index categories: Supersonic and Hypersonic Flow; Computational Methods; Airbreathing Propulsion.

*Staff Scientist, Research Dept. Member AIAA.

deflection angles, these conditions can no longer be reached. The conditions at the triple points become the Guderley[7] conditions, but the shock configuration remains essentially unchanged, except at the triple point itself. This paper considers only freestream conditions, which allow the von Neumann solution at the triple points.

The computational procedure which has been developed to predict conical, inviscid hypersonic and supersonic corner flowfields, will be outlined. This procedure solves Euler's equations and treats shock waves and contact surfaces as discontinuities satisfying the appropriate jump conditions. The von Neumann triple-point conditions are satisfied exactly. Computational results are compared with available experimental data and the numerical results of other investigators. The effects of geometric perturbations on these solutions are studied and the effects of corner flows on inlet nonuniformities are assessed.

II. Computational Procedure

The basic computational procedures used in the present work follow the guidelines presented by Moretti in Ref. 8. A second-order, finite-differnce marching technique was used to find conical solutions of the steady Euler equations with the marching direction being an iterative coordinate.[9] The coordinate system used is shown in Fig. 3; the z coordinate is the marching direction and is aligned along the internal corner. The x coordinate was chosen in the plane of the horizontal wedge and is normal to z. The third coordinate y is taken normal to both x and z and will be in the plane of the vertical wedge only if the dihedral angle ϕ is 90 deg. If the coordinates x and y are scaled with z (i.e., x/z and y/z), they become conical, self-similar variables. Figure 3 defines the geometric and freestream parameters used. The flow deflections on each wall are varied by changing the freestream flow directions (α and β) for fixed sweepback angles Λ_1, Λ_2, and dihedral angle ϕ. The computational domain is the shaded region of Fig. 4, and is bounded by the corner shock and two wall shocks. The freestream and two-dimensional flows are boundary conditions on the low-pressure side of the appropriate shocks. All of the shock waves satisfy the Rankine-Hugoniot jump conditions, while the contact surfaces inside the computational regime satisfy the continuous pressure and normal velocity conditions.

The iteration starts with an arbitrary flowfield in a plane $z=$ const and proceeds by marching the z direction until the flowfield converges (i.e., becomes invariant with z except for a scale factor). The starting conditions are based on the fact that the pressure in the computational domain is nearly constant in the converged solution. All the computations begin with a constant pressure, given by an empirical formula[10] and an assumed shock and contact shape. Typical calculations take about 600 steps (or iterative cycles) to converge.

The computational domain was mapped, as shown in Fig. 5, using a simple Karman-Trefftz transformation. This mapping has a number of advantages. First, the shock and contact shape can be described simply by a polar coordinate system in the mapped space. Second, the surface boundary conditions on the "vertical" wall can be applied at the same value of mapped $\theta=\pi$ independent of the dihedral angle ϕ. Finally, the radial distribution of grid points is automatically adjusted to concentrate points near the shock system. Figure 5 shows the computational space which is developed from the mapped space by normalizing the radial coordinate between the corner ($r=0$) and the shock system. The angular coordinate θ in region 1 is normalized between the horizontal wall and the first contact, in region 2 between the two contacts, and, finally, in region 3 between the second contact and the vertical wall. This normalization of the mapped space has one drawback—it can, in some sense, reduce the generality of the computational procedure. This procedure assumes that the physical space wave/contact system is similar to that shown in Fig. 5. The wave systems in the cases of compression/expansion and expansion/expansion corners are, of course, different from those of Fig. 5.[5] This drawback is not significant in light of the computational simplifications gained using this procedure. The normalization can be changed for the compression/expansion and expansion/expansion cases.

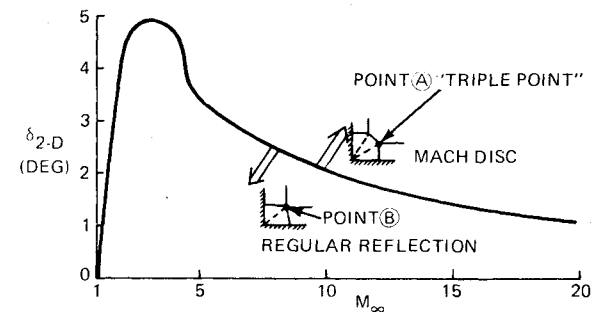

Fig. 2 Maximum deflection for regular reflection (symmetrical wedges).

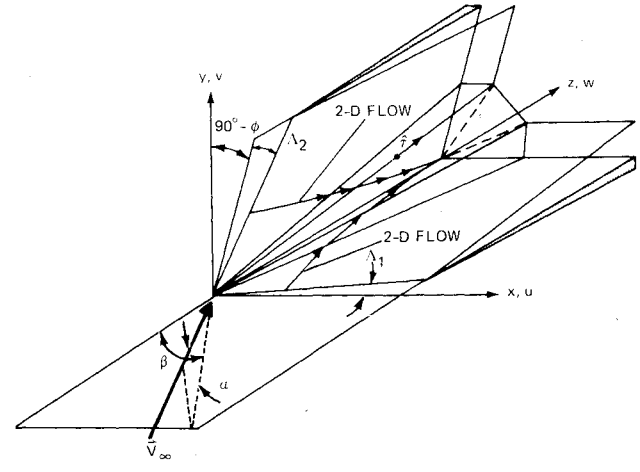

Fig. 3 Corner flow coordiante system.

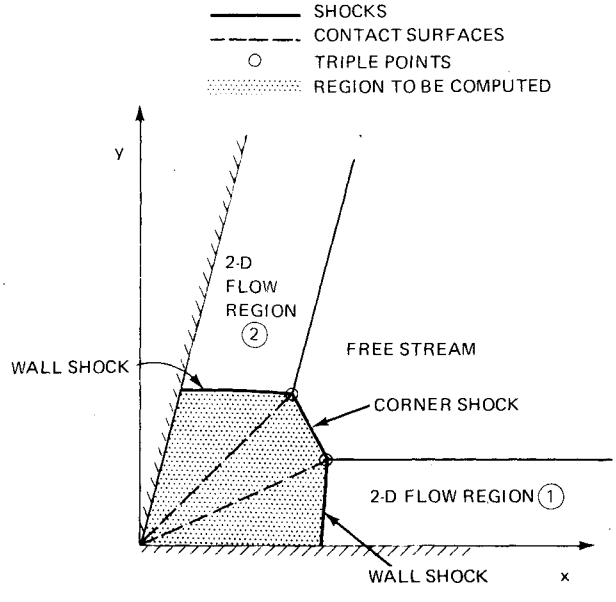

Fig. 4 Shock/contact system, computational domain.

The conditions at the triple points are the von Neumann conditions; that is, matching of pressure and flow deflection on the high-pressure side of the triple points. The flow deflection is matched in a plane normal to a unit vector $\hat{\tau}$ (Fig.

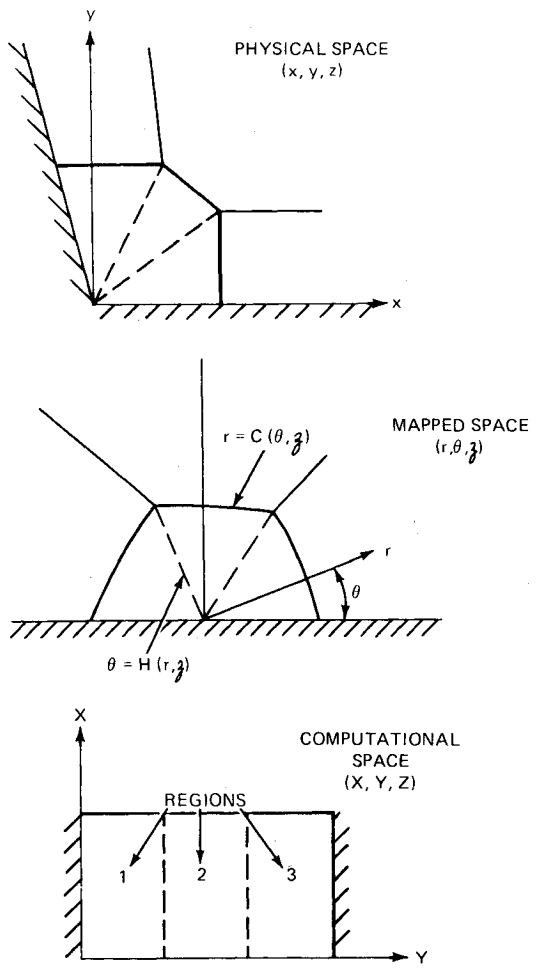

Fig. 5 Mapping of computational domain.

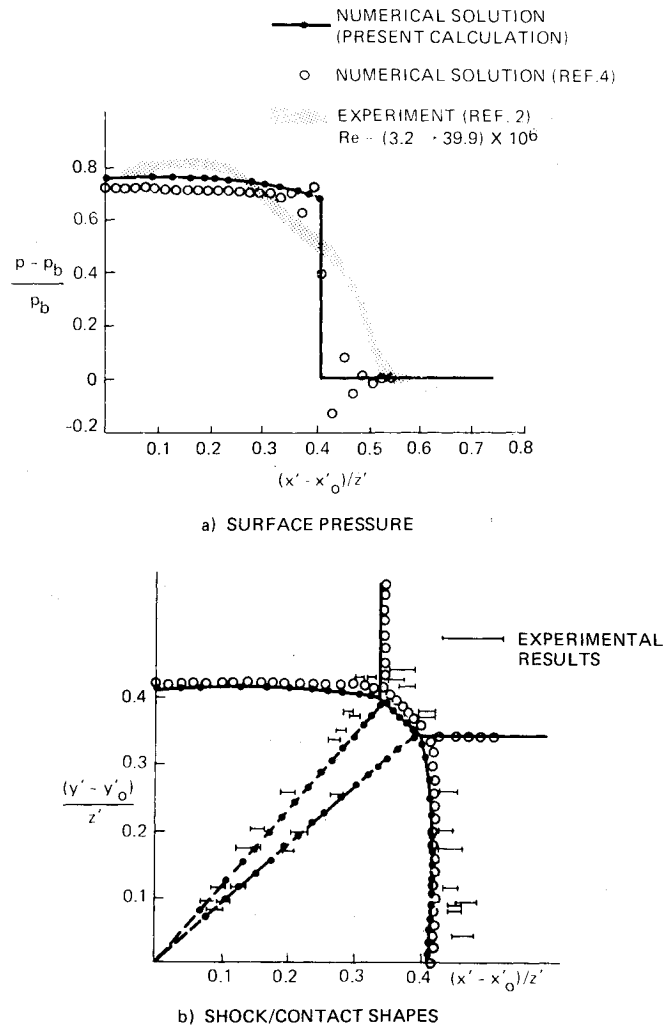

Fig. 6 Comparison with other investigations, symmetrical corner ($M_\infty = 3, \delta_1 = \delta_2 = 9.5, \lambda = 0$).

3) taken along the intersection of the two-dimensional shock and the corner shock. This plane contains the normal to all three shocks and the contact surface at the triple points, and is the proper plane in which to apply the two-dimensional von Neumann conditions.[11,12] As mentioned previously, this paper deals only with freestream conditions and deflection angles which allow for the von Neuman conditions at the triple points. This condition implies $M_\infty > 2$ for deflections larger than 10 deg. The Guderley triple-point condition is singular in that the shocks exhibit infinite curvature at the triple point.[7] Both these singular cases were avoided in the present work because of computational instabilities encountered at the triple points. Reference 5 shows computed results in this range, but it was impossible to assess whether this singularity was captured in these results.

Since the vector $\hat{\tau}$ is constrained to be in the plane of a given two-dimensional shock, only one of its components is free to vary during the iteration. This component ($\hat{\tau}$ component in the z direction) is chosen at each iteration step, so that the conditions at the triple point satisfy the compatibility condition along a characteristic reaching the triple point from inside the flowfield. This condition on the triple point is similar to that imposed on all other shock points. This procedure is repeated as the computation continues in the z (iterative) direction until the unit vector $\hat{\tau}$ and the rest of the flowfield converges. Obviously, at this point $\hat{\tau}$ is in the direction of the conical ray corresponding to the triple point.

The corner itself ($x = y = 0$) (Fig. 3) is a crossflow stagnation point (i.e., $u = v = 0$). It was demonstrated analytically by Salas and Daywitt[13] that this is the only possible stagnation point in this flow. This point is also a vortical singularity since all the crossflow streamlines carry a different entropy. Difficulties associated with this singularity are avoided during the iteration by using a second-order, one-sided difference formula, away from the corner, for the radial derivatives of entropy. As the shock system converges, the entropy behind it becomes constant in the radial direction (the radial direction is nearly the crossflow velocity direction). At this point, the shock entropies are extrapolated to the corner, thus permitting the vortical singularity. The pressure at the corner was computed by satisfying the compatibility conditions along the characteristics reaching the corner on the two intersecting surfaces. The value of pressure at the corner was taken as a weighted average of the values predicted by these characteristics, the weighting being determined by the pressure derivatives.

One area of difficulty encountered during the course of this work was in the computation of the contact surfaces. Originally, the positions of the contacts were integrated in the marching direction with a first-order scheme $H(X,Z+\Delta Z) = H(X,Z) + H_Z \Delta Z$, where H is the mapped polar angle defining the position of the contact and X is a normalized radial coordinate (Fig. 5). It is obvious that the streamlines that wet both sides of the contact surface are generated at the triple point and move down to the corner. With this in mind, the position of the contact was reformulated so that $H(X,Z+\Delta Z) = H(X+\Delta X,Z) + H_Z(X+\Delta X,Z)\,\Delta Z - H_X(X+\Delta X,Z)\Delta X$ where H_Z (as in the previous formulation) is computed by matching pressures on either side of the contact. H_X is evaluated with a second-order formula from the surface position at all points except the

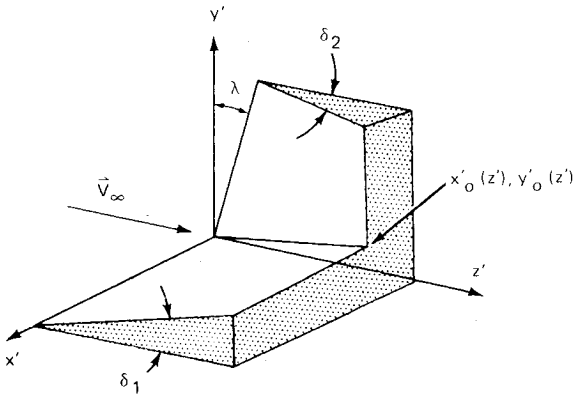

Fig. 7 Freestream fixed coordinate system.

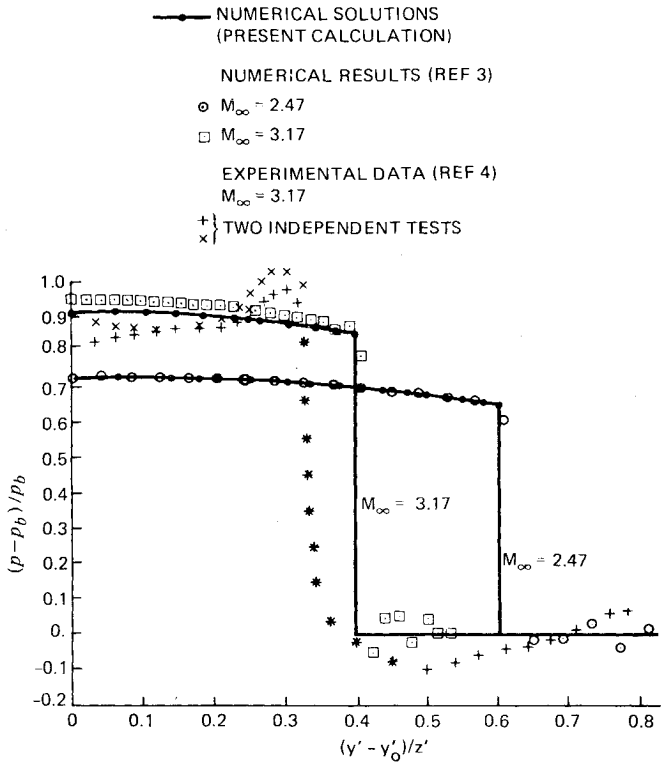

Fig. 8 Comparisons with other investigators, surface pressure ($\delta_1 = \delta_2 = 12.2$ deg, $\lambda = 0$).

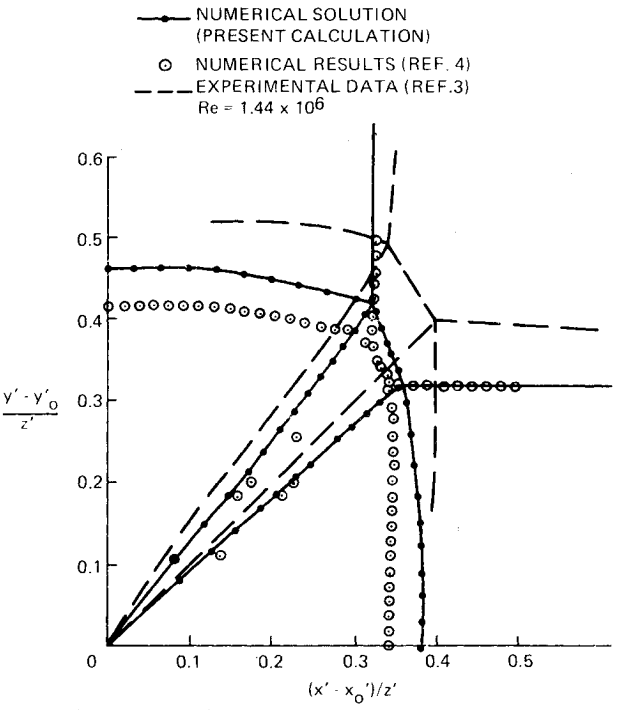

Fig. 9 Comparison of shocks and contacts with other investigators, asymmetrical corner ($M_\infty = 3.17$, $\delta_1 = 3.5$, $\delta_2 = 12.2$ deg, $\lambda = 0$).

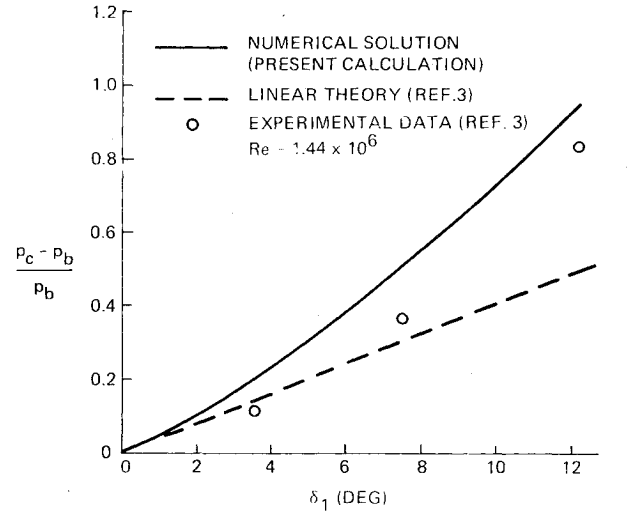

Fig. 10 Effect on corner pressure of varying one-deflection angle ($M_\infty = 3.17$, $\delta_2 = 12.2$ deg, $\lambda = 0$).

triple point where it is computed along with H_Z by matching flow deflection and pressure. This new scheme for locating the position of the contact surface is based on the concept of domain of dependence. Since the streamlines on either side of the contact both originate at the triple point and move down from $X+\Delta X$ to X, the new formulation for surface position corresponds more closely to the correct physical domain of dependence. This stability effect of limiting the numerical domain of dependence was used for a similar problem in Ref. 14.

III. Results

Figure 6 is a comparison of computed results using the present method, the numerical results of Ref. 4, and the experimental results of Ref. 2. The first part of the figure (Fig. 6a) shows surface pressures. The pressure distributions on the vertical and horizontal walls are the same, since the geometry and freestream conditions are symmetrical about the corner diagonal. The coordinates $(x'-x_0')/z'$ and $(y'-y_0')/z'$ are the conical coordinates of Refs. 2 and 4. The coordinates x', y', z' are a freestream-oriented system, such that deflections are produced by δ_1 and δ_2 (Fig. 7). The base pressure p_b is the two-dimensional pressure on either wedge. The results of the present calculations compare quite well with those of Refs. 2 and 4 in terms of pressure, shock shape, and contact surface shape. The numerical results of Ref. 4 exhibit pressure oscillations near the shock which seem to be typical of the computational procedure used (i.e., shock capturing). The same oscillations can be found in Refs. 5 and 6.

Figure 8 is a comparison with the experimental results of Ref. 3 and again the numerical results of Ref. 4. In this comparison, the freestream fixed-coordinate system was used. The figure shows the surface pressure at both $M_\infty = 2.47$ and 3.17 (the experimental pressure at $M_\infty = 2.47$ is unavailable). Both these results are for symmetrical configurations ($\delta_1 = \delta_2 = 12.2$ deg, $\lambda = 0$); again, p_b is the two-dimensional pressure on either wedge. A comparison of Figs. 6 and 8 indicates that both of the inviscid computations presented compare more favorably with the experimental data of Ref. 2 than that of Ref. 3. This is due to the fact that the data of Ref.

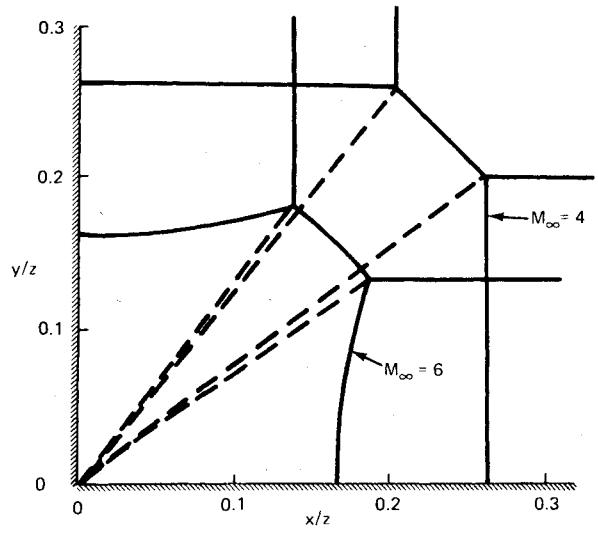

Fig. 11 Effect of Mach number on shocks and contacts ($\alpha = 9.85$ deg, $\beta = 10$ deg, $\Lambda_1 = \Lambda_2 = 0$, $\phi = 90$ deg).

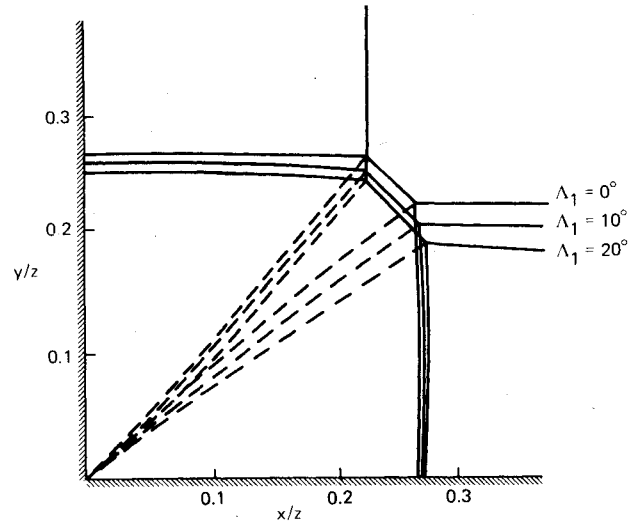

Fig. 12 Effect of sweepback on shocks and contacts ($M_\infty = 4$, $\alpha = 9.85$ deg, $\beta = 10$ deg, $\Lambda_2 = 0$, $\phi = 90$ deg).

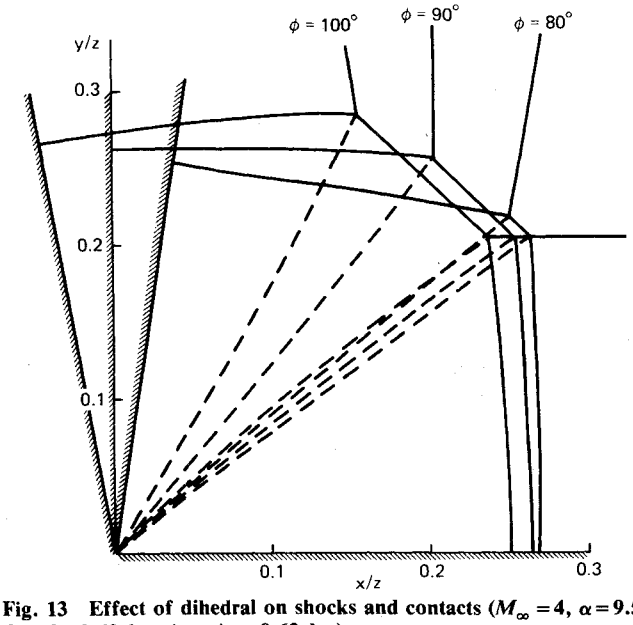

Fig. 13 Effect of dihedral on shocks and contacts ($M_\infty = 4$, $\alpha = 9.5$ deg, $\beta = 9.63$ deg, $\Lambda_1 = \Lambda_2 = 9.63$ deg).

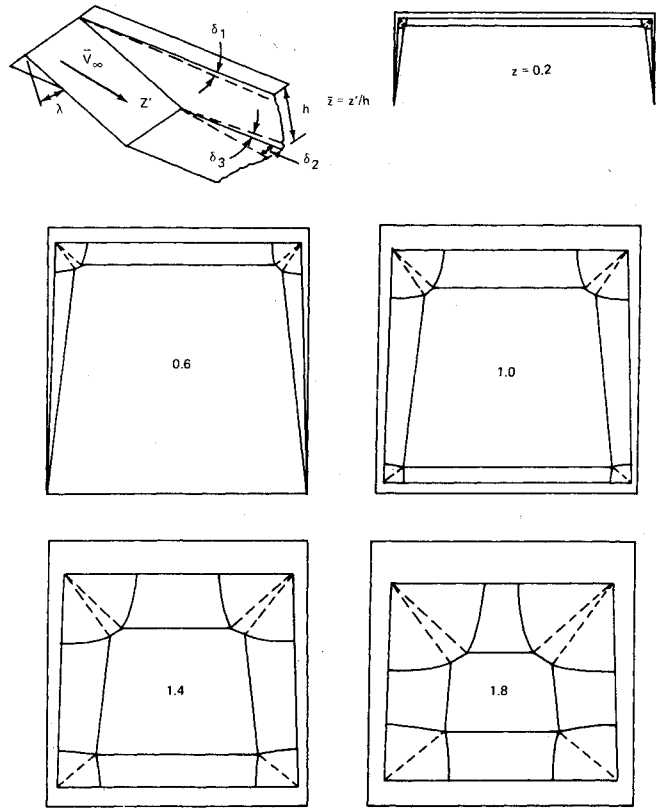

Fig. 14 Hypersonic inlet configuration shock pattern ($M_\infty = 6$, $\delta_1 = \delta_3 = 5$ deg, $\delta_2 = 2.5$ deg, $\lambda = 30$ deg).

2 included higher Reynolds number flows than that of Ref. 3.

Figures 9 and 10 show comparisons with experimental data for asymmetric configurations. Figure 9 is a comparison with the results of Refs. 3 and 4; the vertical and horizontal walls having deflections of $\delta_2 = 12.2$ deg and $\delta_1 = 3.4$ deg, respectively. This figure shows the distortion in the shock system due to the asymmetry. In this case, the results of the present calculations are somewhat different than the numerical results of Ref. 4. Figure 10 shows the variation in the pressure at the corner itself (x_0', y_0' of Fig. 7) when the deflection of one wall, δ_1, is varied while the other, δ_2, is held fixed. The pressure at the corner is normalized with respect to the two-dimensional pressure of the fixed wedge, δ_2. Also shown in this figure are the experimental data of Ref. 3 and the results of first-order linear theory. The comparison between the current results and experiment is acceptable over the range $\delta_1 = 0$ to $\delta_1 = 12.2$ deg. It can be seen that the linear theory underpredicts the pressure significantly at the higher deflections.

Figure 11 compares the computed shock shapes for similar wedge configurations with freestream Mach numbers of 4 and 6. Figure 12 compares the shock and contact systems for three configurations with different horizontal wedge sweepback angles. Figure 13 shows the effect on the shock system of varying the dihedral angle ϕ between the two walls from 100 to 80 deg. Figures 11-13 are all plotted in terms of the corner-fixed coordinate system of Fig. 3.

In an effort to access the impact of conical corner flows on inlet performance, computations of the upper- and lower-corner flowfields of a number of inlet configurations were made. Figure 14 shows the computed shock and contact system for a Mach 6 inlet. These flows are conical, so that each plane $\bar{z} = \text{const}$ ($\bar{z}$ is normalized with respect to the inlet height and $\bar{z} = 0$ at the inlet forward lip) is generated by scaling the conical results. The last cross section in the figure ($\bar{z} = 1.8$) shows how the corner flows dominate large portions of the inlet cross section. The lower corner is a regular reflection pattern in this case. From this figure it can be seen that the

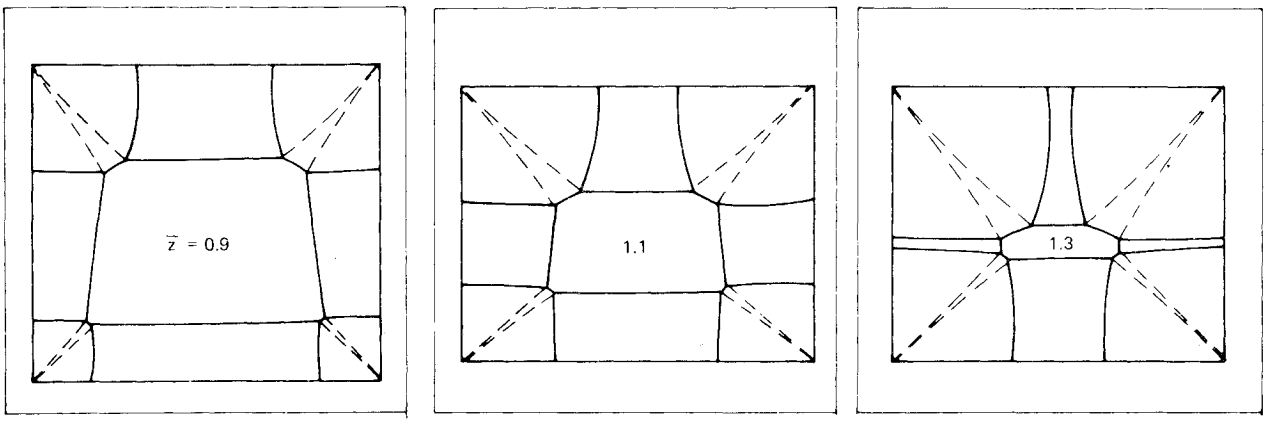

a) SHOCKS/CONTACTS

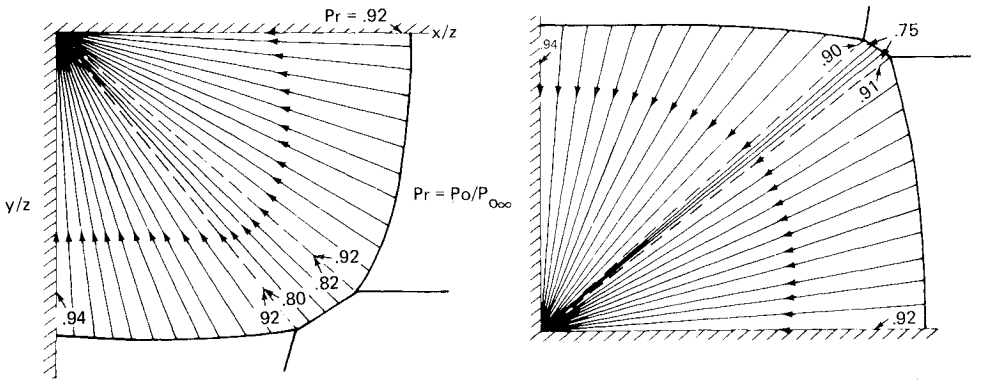

b) TOTAL PRESSURE

Fig. 15 Hypersonic inlet configuration ($M_\infty = 4$, $\delta_1 = \delta_3 = 10$ deg, $\delta_2 = 2.5$ deg, $\lambda = 30$ deg).

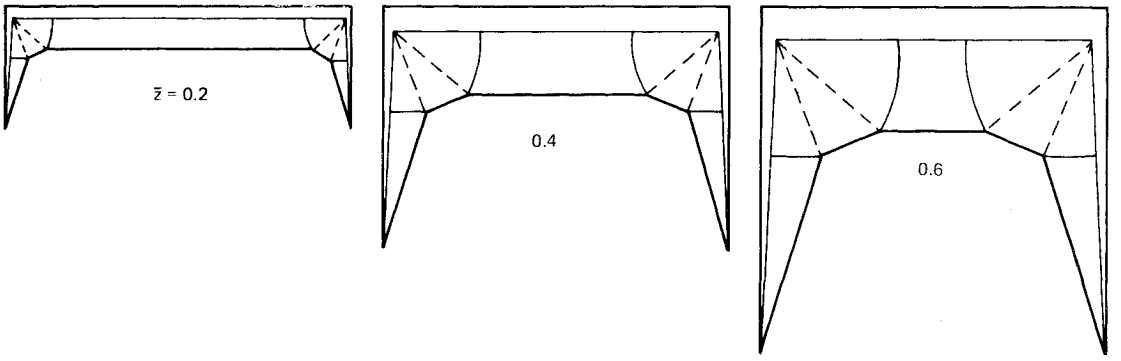

a) SHOCKS/CONTACTS

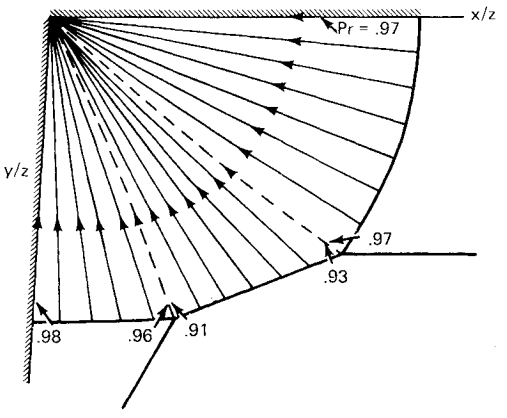

b) TOTAL PRESSURE

Fig. 16 Supersonic inlet configuration ($M_\infty = 2.5$, $\delta_1 = 10$ deg, $\delta_2 = 4.3$ deg, $\lambda = 30$ deg).

nonuniformities generated by the corners will greatly affect the inlet flow. Figure 15 shows the shocks and contacts for a Mach 4 inlet configuration at a number of stations. The last station shown in this case is at $z = 1.3$ inlet heights from the forward lip, the corner flow engulfs most of the inlet cross section. Figure 15b shows the crossflow streamline pattern for both the upper and lower corners. The streamlines are lines of constant entropy and, therefore, of constant total pressure. In Fig. 15b a number of the streamlines are labeled with their total pressure; the large nonuniformities in this quantity are obvious. The inlets of both Figs. 14 and 15 are intended to represent ram/scramjet inlets, so that the corner flows (with their inherent nonuniformities) will be essentially unaltered until the combustion chamber, where they may cause nonuniform combustion. Figure 16a shows a number of cross-sectional shock patterns for a Mach 2.5 inlet. The inlet is assumed to be an all-external compression inlet; $\bar{z} = 0.6$ is the station at which the inlet normal shock might be located. At this station, the corner flow shock pattern will interact with the normal shock but the flow nonuniformities will be transmitted to the compressor face. In this case, as in the higher Mach number cases, the corner flowfields occupy a substantial portion of the inlet. Figure 16b shows the crossflow streamlines and total pressure. In this case, the total pressure losses are smaller than the two previous cases but still important to inlet performance.

Most of the results shown here were computed with a 15×30 (radial $\times$ circumferential) grid and took about 600 steps to converge. Typical running times were about 15 min on an IBM 370/168 computer.

IV. Concluding Remarks

While the basic computational procedure used in this work is somewhat standard, the formulation of the triple-point and the contact surface computations are new and important from the standpoint of numerical analysis. The comparisons with experimental data and the numerical results of Ref. 4 indicate that this computational procedure is sound.

The combination of corner flowfields to form the inlet-like flowfields of Figs. 14-16, indicate that large portions of inlet flows are dominated by the conical flows originating at the corners. A complete inlet flowfield can only be predicted with a fully three-dimensional computation involving the complex problems associated with the interaction of two triple points.

Acknowledgment

This work was supported in part by NASA/LRC under contract NAS1-14162. The author gratefully expresses his appreciation to S. Rudman and P. Del Guidice of the Grumman Research Department and M.D. Salas of NASA Langley Research Center for their helpful discussion on various aspects of this work.

References

[1] Wallace, J. and Clarke, J., "Uniformly Valid Second Order Solution to Supersonic Flow Over Cruciform Surfaces," *AIAA Journal*, Vol. 1, Jan. 1963, pp. 179-185.

[2] West, J. E. and Korkegi, R. H., "Interaction in the Corner of Intersecting Wedges at a Mach Number of 3 and High Reynolds Numbers," *AIAA Journal*, Vol. 10, May 1972, pp 652-656.

[3] Charwat, A. F. and Redekeopp, L. G., "Supersonic Interference Flow Along the Corner of Intersecting Wedges," *AIAA Journal*, Vol. 5, March 1967, pp. 480-488.

[4] Kutler, P., "Numerical Solution for the Inviscid Supersonic Flow in the Corner Formed by Two Intersecting Wedges," AIAA Paper 73-675, 1973.

[5] Anderson, D. A. and Nangia, R. K., "Comparison of Numerical and Experimental Conical Flow Fields in Supersonic Corners with Compression and/or Expansion," *Aeronautical Quarterly*, Vol. 28, Nov. 1977, pp. 293-306.

[6] Shankar, V., Anderson, D., and Kutler, P., "Numerical Solutions for Supersonic Corner Flow," *Journal of Computational Physics*, Vol. 17, Feb. 1975, pp. 160-180.

[7] Sternberg, J., "Triple-Shock-Wave Interactions," *The Physics of Fluids*, Vol. 2, No. 2, March 1959, pp. 179-206.

[8] Moretti, G., Grossman, B., and Marconi, F., "A Complete Numerical Technique for the Calculation of Three-Dimensional Inviscid Supersonic Flows," AIAA Paper 72-192, 1972.

[9] Marconi, F. and Siclari, M., "A Study of the Invsicid Flow about Conically Cambered Delta Wings," AIAA Paper 78-58, Jan. 1978.

[10] Ferri, A., Dash, S., and Del Guidice, P., "Methodology for Three-Dimensional Nozzle Design," NASA CR-132438, March 1974.

[11] Rudman, S., "Three-Dimensional Shock Wave Interactions," AIAA Paper 79-0137, 1979.

[12] Hunt, B. L. and Lamont, P. J., "The Confluence of Three Shock Waves in Three-Dimensional Flow," *Aeronautical Quarterly*, Vol. 29, Feb. 1978, pp. 18-27.

[13] Salas, M. D. and Daywitt, J., "Structure of the Conical Flow Field About External Axial Corners," *AIAA Journal*, Vol. 17, Jan. 1978, pp. 41-47.

[14] Moretti, G. and Pandolfi, M., "Entropy Layers," *Journal of Computers and Fluids*, Vol. 1, No, 19, 1973, pp. 19-35.